Asian Journal of Chemistry; Vol. 38, No. 8 (2026), 2177-2182
ASIAN JOURNAL OF CHEMISTRY
https://doi.org/10.14233/ajchem.2026.36362

Synthesis, Characterisation and Microbial Activity of *Melia azedarach* Encapsulated ZIF-8 Metal-Organic Frameworks

RAJU POTNURU[1,2], GOPI MAMIDI[1,*], TIRUMALA SANTHOSHKUMAR SARIPALLI[3], MARY SHAMYA AROKIARAJAN[3] and ACHINTYA KUMAR MANDAL[3]

[1]Department of Chemistry, V.S. Krishna Government Degree and P.G. College (Affiliated to Andhra University), Visakhapatnam-530013, India
[2]Department of Chemistry, M.R. College (Autonomous), Vizianagaram-535002, India
[3]Regional Research Institute of Unani Medicine, Chennai-600013, India

*Corresponding author: E-mail: drgopichem@gmail.com

Received: 3 May 2026 *Accepted*: 21 July 2026 *Published online*: 7 August 2026 AJC-22445

Zeolite imidazolate frameworks-8 (ZIF-8) is one of the most widely studied metal-organic frameworks (MOFs) due of its high stability, large surface area and excellent gas separation performance. This study reports the encapsulation of the *Melia azedarach* L. extract (MAZ) into zeolitic imidazolate framework-8 (ZIF-8) through a simple nanoprecipitation method. The resulting MAZ@ZIF-8 nanocomposite was characterized by powder X-ray diffraction (PXRD), Fourier-transform infrared (FT-IR) spectroscopy, and dynamic light scattering (DLS). The nanocomposite exhibited good structural stability, remaining stable for at least 25 days, indicating its suitability as a robust functional material. The antimicrobial activities of MAZ, ZIF-8 and MAZ@ZIF-8 were evaluated and compared. The enhanced stability and biological activity of MAZ@ZIF-8 suggest its potential for a wide range of biomedical and antimicrobial applications.

Keywords: ZIF-8, *Melia azedarach*. L, Metal organic frameworks, Nanocomposites, P-XRD.

INTRODUCTION

Melia azedarach L. (Meliaceae), commonly known as Indian or Persian lilac, is a medicinal plant widely distributed in tropical and subtropical regions. It is a rich source of bioactive phytochemicals, including alkaloids, flavonoids, phenolics, tannins, limonoids, triterpenoids, glycosides and sterols, which contribute to its diverse pharmacological properties [1-4]. Extracts of *M. azedarach* have demonstrated a broad spectrum of biological activities including antiviral, antibacterial, antioxidant, antiparasitic, antiplasmodial, anticancer, antihyperglycaemic and cytotoxic effects [5-12]. These therapeutic properties make *M. azedarach* an attractive natural candidate for encapsulation into metal-organic frameworks to improve its stability, controlled release and antimicrobial efficacy.

Metal-organic frameworks (MOFs) are porous crystalline materials that have attracted considerable interest for applications in gas storage, separation, catalysis, sensing, energy storage and biomedicine owing to their high surface area, tunable pore structure and large loading capacity [13]. Their well-defined porous architecture enables the efficient encapsulation of functional molecules, making them promising carriers for therapeutic and bioactive compounds [14,15].

Zeolitic imidazolate framework-8 (ZIF-8), a zinc-based MOF constructed from Zn^{2+} ions and 2-methylimidazole, has emerged as one of the most extensively investigated MOFs due to its high chemical stability, biocompatibility and ease of synthesis. It has been widely explored for adsorption [16,17], membrane separation [18], catalysis [19], biomedical imaging [20] and drug delivery [21]. It has been successfully employed to encapsulate the therapeutic agents including vancomycin, doxorubicin, ciprofloxacin and gentamicin [22-24]. The functional modification of ZIF-8, such as Cu^{2+} doping combined with curcumin loading, has further enhanced its antibacterial performance [25].

Despite these advances, the encapsulation of *M. azedarach* (MAZ) fruit extract in ZIF-8 has received little attention. In this study, a MAZ@ZIF-8 nanocomposite was synthesised by a simple nanoprecipitation method to improve the stability and bioavailability of the plant extract while preserving its

antimicrobial activity. The nanocomposite was characterised by powder X-ray diffraction (PXRD) to confirm phase formation and crystallinity, Fourier-transform infrared (FT-IR) spectroscopy to verify successful encapsulation, dynamic light scattering (DLS) to determine particle size and scanning electron microscopy (SEM) to examine particle morphology. The antimicrobial activity of MAZ, ZIF-8 and MAZ@ZIF-8 was evaluated to assess the effect of encapsulation. The developed nanocomposite provides a simple and sustainable approach for incorporating plant-derived bioactive compounds into MOFs and demonstrates potential for antimicrobial, drug delivery and other biomedical applications.

EXPERIMENTAL

Plant materials: Fresh fruits of *M. azedarach* L. were collected from the local orchard of Vizianagaram District, India, during August, 2025. The plant material was taxonomically authenticated by Dr. Venkatesan, Botanist, Regional Research Institute of Unani Medicine, Chennai, India.

Soxhlation method: Dried *M. azedarach* L. fruit powder (25 g) was placed in a thimble and extracted with 150 mL of ethanol using a Soxhlet apparatus at 75 ºC for 48 h. The resulting extract was filtered through Whatman No. 1 filter paper (180 μm) and the filtrate was kept at room temperature until complete evaporation of the solvent to obtain the crude *M. azedarach* extract (MAZ).

Qualitative phytochemical analysis: Preliminary phytochemical screening of *M. azedarach* L. fruit extracts was performed to detect the presence of amino acids, carbohydrates, reducing sugars, steroids, cardiac glycosides, phenolics, tannins, terpenoids, alkaloids, flavonoids, saponins and anthrones using standard qualitative methods [26].

Physico-chemical analysis: The quality control of the *M. azedarach* L. fruit extract was performed by determining physico-chemical parameters including ethanol-, hexane- and water-soluble extractive values, total ash, acid-insoluble ash, moisture content, loss on drying, pH (5% aqueous solution), volatile oil content and heavy metal levels according to the standard procedures [27,28].

HPTLC analysis: The ethanolic extract of *M. azedarach* L. fruit performed HPTLC analysis. The analysis was performed utilising a CAMAG HPTLC system (Switzerland) alongside a pre-coated silica gel $60F_{254}$ HPTLC plate (5 cm × 10 cm, Merck, Germany). Sample (5 μL) were applied to the plate utilising a CAMAG ATS4 sample applicator. The mobile phase was composed of toluene, ethyl acetate and formic acid in a ratio of 7:3:0.01. The plates reached a height of 8 cm at room temperature within a CAMAG twin-through glass chamber (10 cm × 10 cm) after a saturation period of 20 min. Following the development process, the plates underwent air-drying at ambient temperature. The chromatographic bands were observed with the CAMAG UV Visualizer 2 at wavelengths of 254 nm and 366 nm. The chromatograms underwent scanning with a CAMAG TLC scanner and the R_f values were recorded utilising WINCATS planar chromatography manager software [29].

Synthesis of MAZ@ZIF-8 nanoparticle: The MAZ@ZIF-8 nanocomposite was synthesised by a simple nanoprecipitation method. Initially, 2-methylimidazole (3.3 g, 2 mmol) was dissolved in 50 mL of methanol. $Zn(NO_3)_2 \cdot 6H_2O$ (1.5 g, 2 mmol) was separately dissolved in 50 mL of methanol, after which 10 mL of *M. azedarach* (MAZ) extract was added. The resulting solution was introduced dropwise into the ligand solution under magnetic stirring at 400 rpm and maintained for 1 h to facilitate the formation of the nanocomposite. The precipitated product was recovered by centrifugation at 4000 rpm for 15 min, washed thoroughly with distilled water followed by methanol to remove unreacted species and dried at room temperature. A colourless polyhedral solid (0.258 g) was obtained. The structural and physico-chemical properties of the synthesised MAZ@ZIF-8 were investigated using FT-IR, PXRD, DLS and SEM techniques.

Characterisation: The synthesised MAZ@ZIF-8 nanocomposite was characterized using complementary analytical techniques. Powder X-ray diffraction (PXRD) patterns were recorded on a Bruker Kappa Apex II diffractometer over a 2θ range of 0-90º using Cu*K*α radiation (λ = 1.54060 Å) operated at 40 kV and 35 mA with a scan rate of 0.2 s. Fourier transform infrared (FT-IR) spectra were acquired using a Thermo Nicolet FT/IR-5700 spectrometer. The surface morphology of the nanocomposite was examined by scanning electron microscopy (SEM). Hydrodynamic particle size and zeta potential were determined at room temperature using a Malvern Zetasizer Nano ZS dynamic light scattering (DLS) instrument (Malvern Instruments, UK).

Determination of microbial load: The microbiological quality was evaluated in accordance with the United States Pharmacopeia (USP, 2016) and World Health Organization (WHO, 2007) guidelines. Total aerobic bacterial and fungal counts were determined using 1 g of the sample. The sample was suspended in peptone broth, serially diluted and analysed by the pour plate method in triplicate. Microbial growth was expressed as CFU/g and compared with the WHO permissible limits. The samples with microbial counts exceeding 10^5 CFU/g were considered unsuitable for further evaluation.

Determination of bacteria: Pathogenic bacteria were identified following standard microbiological procedures. The samples were suspended in peptone water, homogenized thoroughly and serially diluted before inoculation onto selective media. MacConkey agar, eosin methylene blue (EMB) agar, cetrimide agar and mannitol salt agar were used for the isolation of *Escherichia coli*, *Pseudomonas aeruginosa*, *Salmonella* spp. and *Staphylococcus aureus*, respectively. Following incubation, the isolates were identified based on colony morphology, Gram staining and biochemical tests including oxidase, catalase and gas production assays.

RESULTS AND DISCUSSION

The phytochemical composition of *M. azedarach* L. fruit extracts is shown in Table-1. The ethanolic extract contained the highest abundance of bioactive constituents, including alkaloids, phenolics, flavonoids, triterpenoids, tannins, sterols, quinones and coumarins, whereas the chloroform and hydroalcoholic extracts exhibited comparatively lower phytochemical content. The predominance of alkaloids is noteworthy due to their well-documented pharmacological activities including

TABLE-1
PHYTOCHEMICAL ANALYSIS OF THE PLANT EXTRACT

Tests	Ethanol	Chloroform	Hydro alcohol
Alkaloids	++	+	++
Phenols	++	–	–
Flavonoids	++	–	–
Terpenoids	–	–	–
Triterpenoids	++	–	–
Tannins	++	–	+
Saponins	–	+	++
Sterols	++	+	+
Quininies	++	+	+
Coumarins	+	–	+
Liginins	–	–	–
Proteins	–	–	–
Carbohydrate	+	–	+
Starch	–	–	–

antioxidant, anti-inflammatory, antidiabetic and antibacterial effects, which contribute to the therapeutic potential of the extract [30].

Physico-chemical studies: The physico-chemical quality control parameters of *M. azedarach* L. fruit are shown in Table-2. These values can be used as reference data for assessing the quality and authenticity of the plant material and for identifying adulterated or poor-quality samples. Loss on drying represents the moisture content of the sample, while total ash and acid-insoluble ash reflect its mineral content and the presence of inorganic contaminants. The extractive values obtained with ethanol, water and hexane indicate the number of soluble constituents present in each solvent. The pH of the aqueous extract was determined to assess its chemical nature. These findings provide baseline data for the identification and quality evaluation of *M. azedarach* fruit.

TABLE-2
PHYSIO-CHEMICAL PARAMETERS OF *M. azedarach* L. FRUIT

Content	Observation
% of loss of drying	9.63%
% of total ash	5.90%
% of acid insoluble ash	0.62%
% of alcohol soluble extractive value	2.59%
% of hexane soluble extractive value	16.19%
% of water-soluble extractive value	1.62%
pH	5.97

HPTLC analysis: The HPTLC fingerprint profile of *M. azedarach* L. fruit is shown in Fig. 1. Densitometric scanning at 254 nm resolved 14 peaks with R_f values of 0.11 (1.74%), 0.16 (0.69%), 0.19 (2.11%), 0.27 (6.60%), 0.31 (10.23%), 0.42 (2.10%), 0.48 (6.24%), 0.51 (7.08%), 0.59 (3.52%), 0.69 (4.96%), 0.73 (0.85%), 0.86 (4.15%), 0.92 (13.37%) and 0.98 (36.33%). At 366 nm, three major peaks were observed at R_f values of 0.31 (86.09%), 0.94 (2.10%) and 0.98 (11.82%). The distinct chromatographic pattern confirms the presence of multiple phytochemical constituents in the extract. The HPTLC fingerprint and corresponding 3D densitograms (Figs. 2-5) provide a characteristic chromatographic profile that can be used as a reference for the authentication and quality assessment of *M. azedarach* fruit [31].

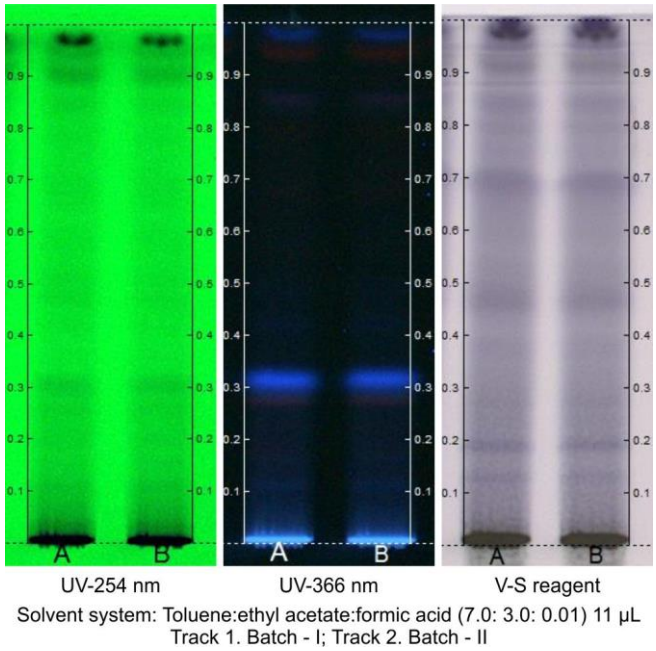

Fig. 1. Various UV wavelength HPTLC fingerprint of *M. azedarach* L. fruit (alcohol extract)

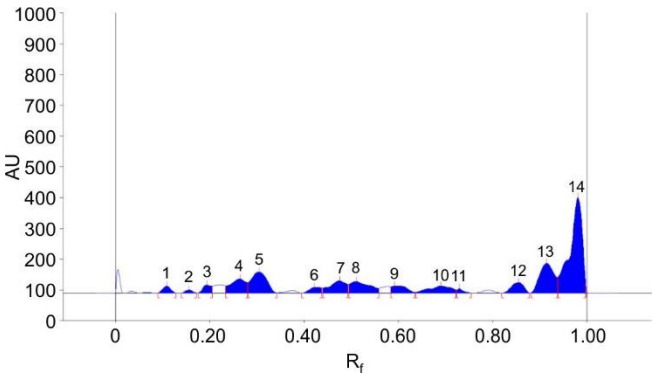

Fig. 2. HPTLC fingerprint of *M. azedarach* (fruit) in alcohol extract at 254 nm (absorbance mode)

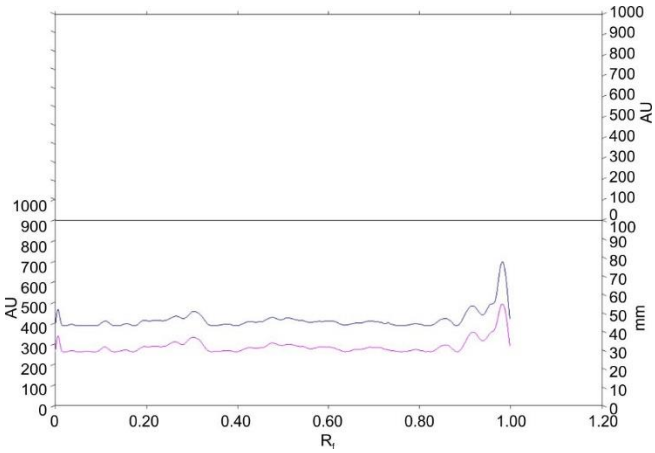

Fig. 3. Densitometric chromatogram of *M. azedarach* (fruit) in alcohol extract at 254 nm (absorbance mode)

PXRD studies: PXRD study of MAZ@ZIF-8 was performed to assess the crystalline structure of *M. azedarach* L. fruit extract (MAZ), pure ZIF-8 and the synthesised MAZ@ZIF-8 nanocomposite. The XRD patterns of ZIF-8 exhibited

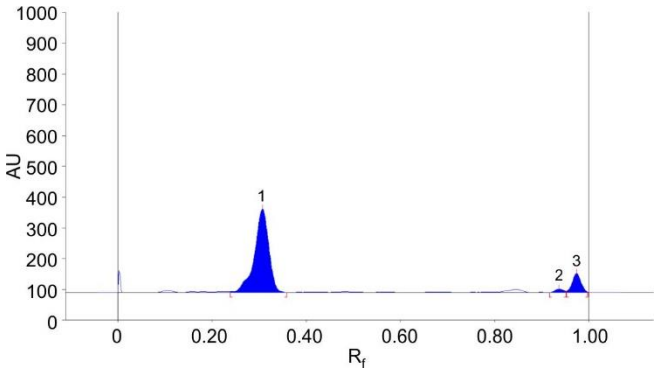

Fig. 4. HPTLC fingerprint of *M. azedarach* (fruit) in alcohol extract at 366 nm (fluorescence mode)

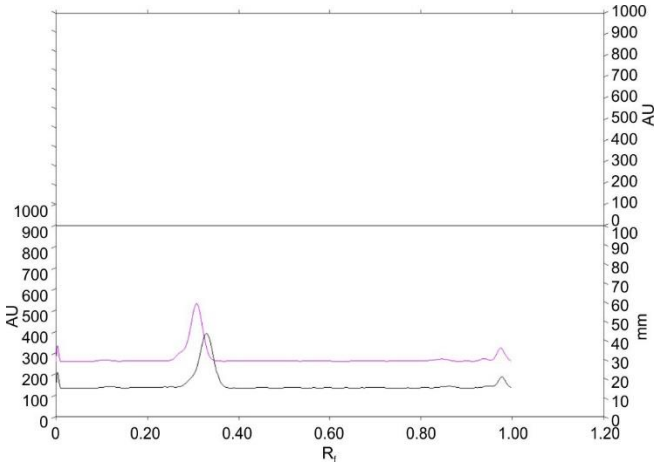

Fig. 5. Densitometric chromatogram of *M. azedarach* (fruit) in alcohol extract at 366 nm (fluorescence mode)

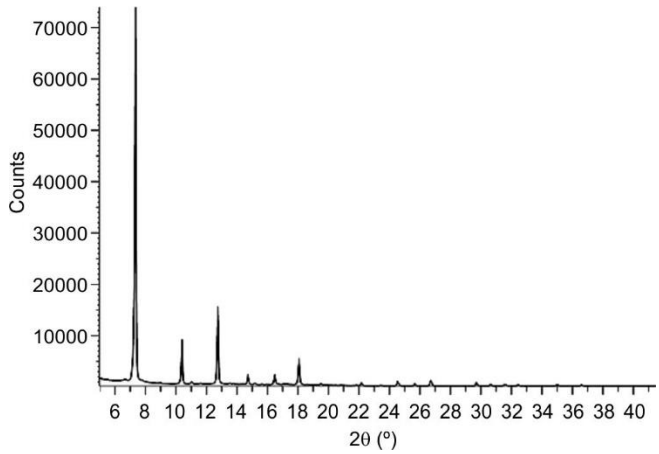

Fig. 6. PXRD spectrum of MAZ@ZIF-8 MOF

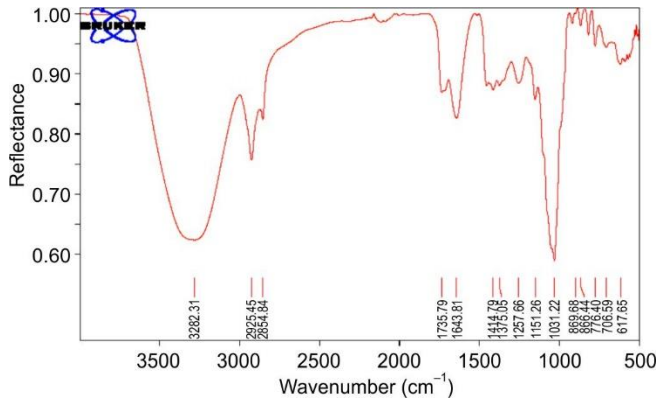

Fig. 7. FT-IR spectrum of MAZ@ZIF-8 MOF

sharp peaks at 2θ values of 7.26º, 10.52º, 12.96º, 14.94º, 16.44º and 18.02º corresponding to the crystallographic planes (110), (200), (211), (022), (013) and (222), respectively. The PXRD pattern of MAZ@ZIF-8 (Fig. 6) exhibited the characteristic diffraction peaks of ZIF-8, which is consistent with the reported data [32]. The absence of additional diffraction peaks and the retention of the original peak positions indicate that encapsulation of MAZ extract did not alter the crystalline framework of ZIF-8. These results confirm the successful formation of a phase-pure MAZ@ZIF-8 nanocomposite with preserved crystallinity. Since PXRD alone cannot distinguish encapsulation within the pores from surface adsorption, the diffraction data were interpreted together with the FT-IR results. The FT-IR spectrum exhibited characteristic absorption bands of both ZIF-8 and the MAZ extract, together with slight band shifts that are consistent with interactions between the extract constituents and the framework. The combined PXRD and FT-IR analyses establish successful incorporation of the extract without altering the structural integrity of the ZIF-8 framework, making the material suitable for antimicrobial and biomedical applications [33].

FTIR studies: FT-IR spectrum (Fig. 7) displayed absorption bands at 3282, 2928, 2854, 1739, 1643, 1382, 1258, 1152, 1031, 866, 797, 756, 693, 630 and 578 cm^{-1}. The broad band centred at 3282 cm^{-1} is assigned to O–H and N–H stretching vibrations of hydroxyl- and amine-containing constituents of the MAZ. The bands at 2928 and 2854 cm^{-1} correspond to the asymmetric and symmetric stretching vibrations of aliphatic C–H groups. The absorption at 1739 cm^{-1} is attributed to C=O stretching of carbonyl-containing phytoconstituents, while the band at 1643 cm^{-1} is due to the N–H bending and/or the bending vibration of adsorbed water, with possible contribution from conjugated carbonyl groups. The bands at 1382, 1258 and 1152 cm^{-1} are associated with C–N and C–O stretching vibrations of the imidazolate linker and plant-derived constituents. The intense absorption at 1031 cm^{-1} is characteristic of C–N stretching of the ZIF-8 framework with overlap from C–O stretching of the encapsulated extract. The bands observed at 866, 797, 756, 693, 630 and 578 cm^{-1} are assigned to imidazolate ring vibrations and Zn–N stretching modes, confirm the formation of the ZIF-8 framework. The FT-IR spectrum contained the characteristic absorption bands of both the MAZ and the ZIF-8 framework. Small shifts in several bands suggest interactions between the phytochemical constituents and the framework. The FT-IR and PXRD results show that the extract was incorporated into ZIF-8 while the crystalline framework remained unchanged.

DLS studies: The stability of MAZ@ZIF-8 nanoparticles was assessed over 25 days of storage. No precipitation or appreciable change in particle size was observed throughout the study. DLS analysis (Fig. 8) showed that most particles were distributed between 155 and 170 nm, with the largest fraction falling within the 165-170 nm range. The narrow particle size distribution reflects the formation of relatively uniform nanoparticles.

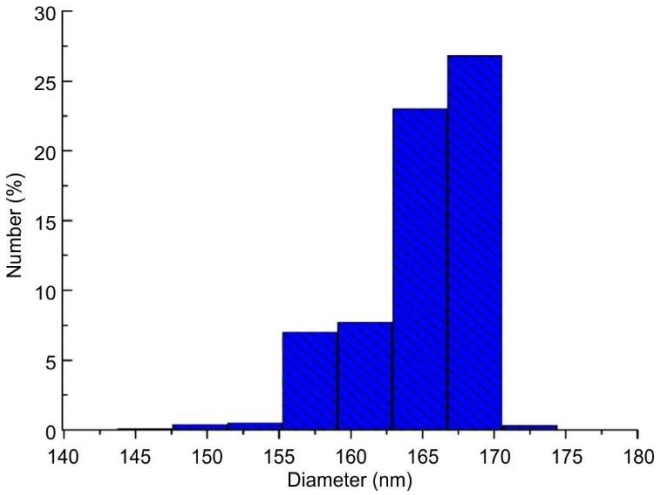

Fig. 8. Particle size distribution of MAZ@ZIF-8 nanoparticles after 25 days of storage determined by DLS

SEM studies: The morphology of MAZ@ZIF-8 was examined by SEM and compared with that of pure ZIF-8. As shown in Fig. 9a-b, both samples exhibited the characteristic condensed rhombic dodecahedral morphology of ZIF-8 crystals. The SEM images showed particles with well-defined facets, sharp edges, and smooth surfaces, consistent with the formation of highly crystalline ZIF-8. No noticeable change in particle morphology was observed after incorporation of the MAZ and the characteristic structure of ZIF-8 remained intact. These observations agree with the previous reports on ZIF-8 crystals [34,35] and support the preservation of the framework during synthesis.

Microbial load of MAZ@ZIF-8: The microbiological quality of the synthesised MAZ@ZIF-8 nanocomposite was evaluated to assess its suitability for subsequent biological and pharmaceutical studies. The total bacterial count was 1×10^4 CFU/g, while the total fungal count was below 1 CFU/g, both of which fall within the acceptable limits prescribed by pharmacopeial and WHO guidelines. The microbiological analysis further confirmed the absence of common pathogenic microorganisms, *viz. E. coli*, *Salmonella* spp., *S. aureus*, *P. aeruginosa* and some members of the *Enterobacteriaceae* family. The low microbial load and absence of pathogenic contaminants reflect good microbiological quality of the synthesized nanocomposite and indicate that the preparation process was carried out under appropriate hygienic conditions. These findings support the use of MAZ@ZIF-8 in further antimicrobial, biomedical and pharmaceutical investigations, where microbiological purity is an essential requirement.

Conclusion

A MAZ@ZIF-8 nanocomposite was synthesised by a simple and straightforward green nanoprecipitation method using the ethanolic extract of *Melia azedarach* L. fruit. Phytochemical screening confirmed the presence of alkaloids, phenolics, flavonoids, triterpenoids, tannins, sterols, quinones and coumarins in the extract. Physico-chemical evaluation, HPTLC fingerprinting, and microbial load testing confirmed the quality and authenticity of the plant material. Structural characterization by PXRD, FT-IR, DLS and SEM confirmed the formation of the ZIF-8 framework and the incorporation

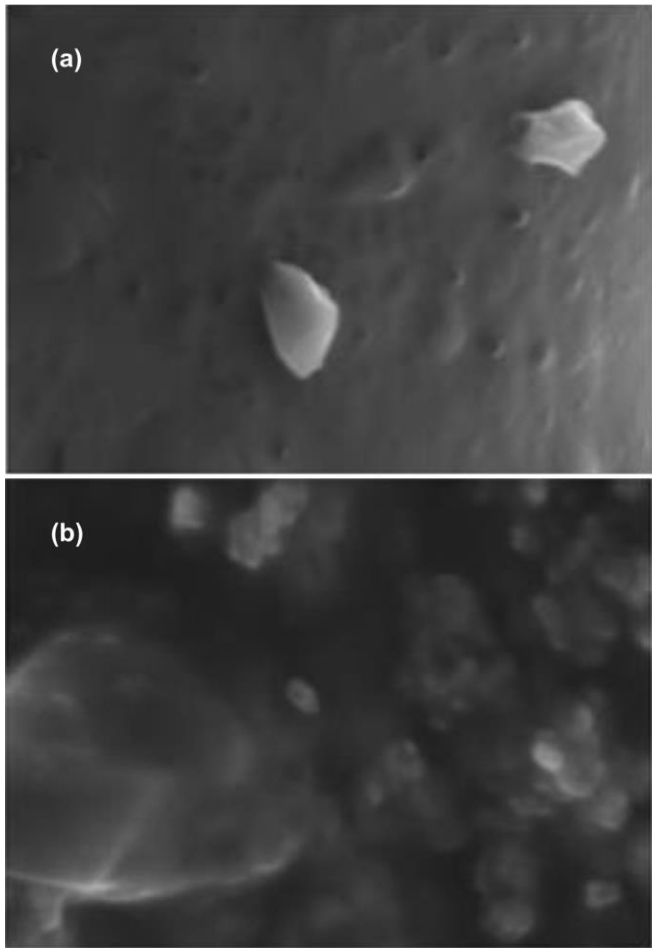

Fig. 9. SEM images of MAZ@ZIF-8

of the plant extract without altering the crystalline morphology of the host material. The synthesised nanocomposite exhibited good colloidal stability, a narrow particle size distribution and the characteristic condensed rhombic dodecahedral morphology of ZIF-8. Microbiological analysis confirmed low bacterial and fungal counts and the absence of pathogenic microorganisms in the prepared nanocomposite.

ACKNOWLEDGEMENTS

The authors express their sincere gratitude to staff of Maharajah's College (Autonomous), Vizianagaram, for financial support and research facilities. Thanks are due to the Assistant Director (Chemistry) and the Director General, Central Council for Research in Unani Medicine (CCRUM), New Delhi, as well as Andhra University, Visakhapatnam, India, for their support and assistance.

CONFLICT OF INTEREST

The authors declare that there is no conflict of interests regarding the publication of this article.

DECLARATION OF AI-ASSISTED TECHNOLOGIES

During the preparation of this manuscript, the authors used an AI-assisted tool(s) to improve the language and no

data, results or scientific conclusions were generated by AI. All analyses, interpretations and conclusions are the authors' own. The authors reviewed and edited the content and take full responsibility for the published work.

REFERENCES

1. A.M.M. Azam, A.N.M. Rashid, N.M. Towfique, M.K. Sen and S. Nasrin, *Am. J. BioSci.*, **1**, 44 (2013); https://doi.org/10.11648/j.ajbio.20130102.13
2. T.T. Hieu, N.T. Chung, V.C. Dung and D.X. Duc, *Curr. Org. Chem.*, **26**, 2160 (2022); https://doi.org/10.2174/1385272827666230130140839
3. W. Fan, J. Li, Y. Huang, X. Wang, and others, *Front. Pharmacol.*, **13**, 829330 (2022); https://doi.org/10.3389/fphar.2022.829330
4. M. Song, H.-J. Luo, Z.-W. Li, L. Qiu, Y.-X. Zhao, C.-W. He, X.-Q. Zhang, W.-C. Ye, L.-G. Lin and Q.-W. Zhang, *Phytochemistry*, **216**, 113869 (2023); https://doi.org/10.1016/j.phytochem.2023.113869
5. N.A.N. Nethmini, M.S. Kim, K. Chathuranga, J.Y. Ma, H. Kim and J.-S. Lee, *J. Biomed. Transl. Res.*, **21**, 125 (2020); https://doi.org/10.12729/jbtr.2020.21.3.125
6. S. Ramya, P.J. Jepachanderamohan, M. Kalayanasundaram, N. Alaguchamy and R. Jayakumararaj, *Ethnobot. Leafl.*, **13**, 254 (2009).
7. N. Vijendra and K.P. Kumar, *Afr. J. Pharm. Pharmacol.*, **4**, 662 (2010).
8. M.C. Corpinella, M. Miranda, W.R. Almiron, C.G. Ferrayoli, F.L. Almeida and S.M. Palacios, *J. Am. Acad. Dermatol.*, **56**, 250 (2007); https://doi.org/10.1016/j.jaad.2006.10.027
9. C.B. Wandscheer, J.E. Duque, M.A.N. da Silva, Y. Fukuyama, J.L. Wohlke, J. Adelmann and J.D. Fontana, *Toxicon*, **44**, 829 (2004); https://doi.org/10.1016/j.toxicon.2004.07.009
10. M.A. Neycee, G.H.A. Nematzadeh, A. Dehestani and M. Alavi, *Int. J. Agric. Crop Sci.*, **4**, 709 (2012).
11. V.D. Szewczuk, E.R. Mongelli and A.B. Pomilio, *Mol. Similarity Med. Chem.*, **1**, 54 (2003).
12. P. Samudram, R. Vasuki, H. Rajeshwari, A. Geetha and P. Sathiya Moorthi, *J. Med. Plants Res.*, **3**, 1078 (2009).
13. D. Li, A. Yadav, H. Zhou, K. Roy, P. Thanasekaran and C. Lee, *Glob. Challenges*, **8**, 2300244 (2024); https://doi.org/10.1002/gch2.202300244
14. C. He, K. Lu, D. Liu and W. Lin, *J. Am. Chem. Soc.*, **136**, 5181 (2014); https://doi.org/10.1021/ja4098862
15. P.-H. Tong, L. Zhu, Y. Zang, J. Li, X.-P. He and T.D. James, *Chem. Commun.*, **57**, 12098 (2021); https://doi.org/10.1039/D1CC05157A
16. H. Li, X.T. Gao, C.Z. Jia, W. Chen, B. Liu, L.Y. Yang, C.Y. Sun and G.J. Chen, *Energies*, **11**, 1890 (2018); https://doi.org/10.3390/en11071890
17. A.A. Jameh, T. Mohammadi, O. Bakhtiari and M. Mandyarfar, *J. Environ. Chem. Eng.*, **7**, 103058 (2019); https://doi.org/10.1016/j.jece.2019.103058
18. A.J. Cruz, G. Arnauts, M. Obst, D.E. Kravchenko, P.M. Vereecken, S. De Feyter, I. Stassen, T. Huffman and R. Ameloot, *Dalton Trans.*, **50**, 6784 (2021); https://doi.org/10.1039/D1DT00927C
19. H. Kargar, M. Ghahramaninezhad, M.N. Shahrak and S.S. Balula, *Micropor. Mesopor. Mater.*, **317**, 110992 (2021); https://doi.org/10.1016/j.micromeso.2021.110992
20. L. Kang, S. Smith and C.Z. Wang, *J. Colloid Interface Sci.*, **588**, 101 (2021); https://doi.org/10.1016/j.jcis.2020.12.068
21. C.L. Hao, D.R. Zhou, J.X. Xu, S. Hong, W.M. Wei, T.T. Zhao, H.B. Huang and W.J. Fang, *J. Mater. Sci.*, **56**, 9434 (2021); https://doi.org/10.1007/s10853-021-05828-y
22. A.A. El-Bindary, E.A. Toson, K.R. Shoueir, H.A. Aljohani and M.M. Abo-Ser, *Appl. Organomet. Chem.*, **34**, e5905 (2020); https://doi.org/10.1002/aoc.5905
23. Y. Wang, Q.J. Ji, J.X. Xu, J. Wan and L. Wang, *Sep. Purif. Technol.*, **276**, 119369 (2021); https://doi.org/10.1016/j.seppur.2021.119369
24. B. Soltani, H. Nabipour and N.A. Nasab, *J. Inorg. Organomet. Polym. Mater.*, **28**, 1090 (2018); https://doi.org/10.1007/s10904-017-0745-z
25. S. Duan, X. Zhao, Z. Su, C. Wang and Y.J. Lin, *ACS Appl. Bio Mater.*, **3**, 3673 (2020); https://doi.org/10.1021/acsabm.0c00300
26. N. Morsy, *Main Group Chem.*, **13**, 7 (2014); https://doi.org/10.3233/MGC-130117
27. W.A.S. Akbar, M.S. Arokiarajan, J.J. Christopher, N.Z. Ahmed and R. Meena, *Biocatal. Agric. Biotechnol.*, **50**, 102745 (2023); https://doi.org/10.1016/j.bcab.2023.102745
28. J.J. Christopher, S.W. Akram, M.S. Arokiarajan, M. Jameel, T.S.K. Saripalli, V.M. Ahmed and K.K. Ahmad, *Food Humanity*, **1**, 100326 (2024); https://doi.org/10.1016/j.foohum.2024.100326
29. M. Kancherla, R. Meena and M.Y. Dar, *J. Herb. Med.*, **42**, 100812 (2023); https://doi.org/10.1016/j.hermed.2023.100812
30. B. Singh, D. Pandya and A. Mankad, *J. Plant Sci. Res.*, **36**, 53 (2020).
31. R. Potnuru, G. Mamidi, T. S. Saripalli, M.S. Arokiarajan, J. Christopher, A.K. Mandal and M. Jameel, *Discover Nano*, **20**, 192 (2025); https://doi.org/10.1186/s11671-025-04377-6
32. N.S. Kumar, M.S. Reddy, T.S. Kumar, V.R. Bheeram, S.B. Mukkamala and L. Chandrasekhara Rao, *ChemistrySelect*, **4**, 1188 (2019); https://doi.org/10.1002/slct.201803302
33. H. Yu, S.S. Muhammad, H. Murtaza, Z. Ayesha, Z. Xi, W. Muhammad, T. Tuba, X. Huang and H. Riaz, *ACS Omega*, **8**, 48535 (2023); https://doi.org/10.1021/acsomega.3c08494
34. J. Bankuru, V.R. Battula, T.S. Santhoshkumar, S. Gopal, R.P. Meena and N.Z. Ahmed, *JCIS Open*, **12**, 100097 (2023); https://doi.org/10.1016/j.jciso.2023.100097
35. X. Meng, K. Jia, K. Sun, L. Zhang and Z. Wang, *Chem. Eng. J.*, **415**, 128947 (2021); https://doi.org/10.1016/j.cej.2021.128947